Journal of Physics: Conference Series **467** (2013) 012009 doi:10.1088/1742-6596/467/1/012009

An ultra-high optical depth cold atomic ensemble for quantum memories

B. M. Sparkes[1], J. Bernu[1], M. Hosseini[1], J. Geng[1,2], Q. Glorieux[1,3], P. A. Altin[4], P. K. Lam[1], N. P. Robins[4], and B. C. Buchler[1].

[1] Centre for Quantum Computation and Communication Technology, Department of Quantum Science, Research School of Physics and Engineering, The Australian National University, Canberra, ACT 0200, Australia
[2] Quantum Institute for Light and Atoms, Department of Physics, East China Normal University, Shanghai 200062, P. R. China
[3] Joint Quantum Institute, University of Maryland, College Park, Maryland 20742, USA
[4] Quantum Sensors Lab, Department of Quantum Science, Australian National University, Canberra, ACT 0200, Australia

E-mail: ping.lam@anu.edu.au

Abstract. Quantum memories for light lie at the heart of long-distance provably-secure communication. Demand for a functioning quantum memory, with high efficiency and coherence times approaching a millisecond, is therefore at a premium. Here we report on work towards this goal, with the development of a ^{87}Rb magneto-optical trap with a peak optical depth of 1000 for the D2 $F = 2 \rightarrow F' = 3$ transition using spatial and temporal dark spots. With this purpose-built cold atomic ensemble we implemented the gradient echo memory (GEM) scheme on the D1 line. Our data shows a memory efficiency of $80 \pm 2\%$ and coherence times up to 195 μs.

1. Introduction

Quantum repeaters are needed to extend the distance of quantum key distribution past its current limit of hundreds of kilometres. A key component of a quantum repeater is a quantum memory. A quantum memory for this application needs to have an efficiency approaching unity without adding noise to the state, and storage times from milliseconds to seconds. Ideally it would also have a high bandwidth and be able to store many pieces of information simultaneously. Many different techniques are currently being developed and much experimental progress has been made over the past few years, with: efficiencies approaching 90% [1]; storage times of over seconds [2, 3]; bandwidths of gigahertz [4, 5]; and over 1000 pieces of information stored at one time [6]. These results were, however, achieved using different memory schemes in different storage media. The challenge now is to reproduce these results with one memory.

Here we will focus on the gradient echo memory (GEM) scheme, which shows great promise due to the high efficiencies achieved in both warm atomic vapours [1] and solid state systems [7]. GEM has also been used to demonstrate temporal compression and stretching of pulses, as well as a capacity to arbitrarily resequence stored information [8] and the interference of initially time-separated pulses [9, 10]. However, the maximum coherence time for GEM to date is 50 μs [11], limited by atomic diffusion in warm vapors.

Motivated by other work demonstrating both high efficiencies [12] and long storage times [3] in cold atomic systems, we introduce a cold atom realisation of GEM. To achieve this we first had to develop an ultra-high optical depth (OD) atomic source to allow for high efficiency recall.

2. Developing the Cold Atomic Source

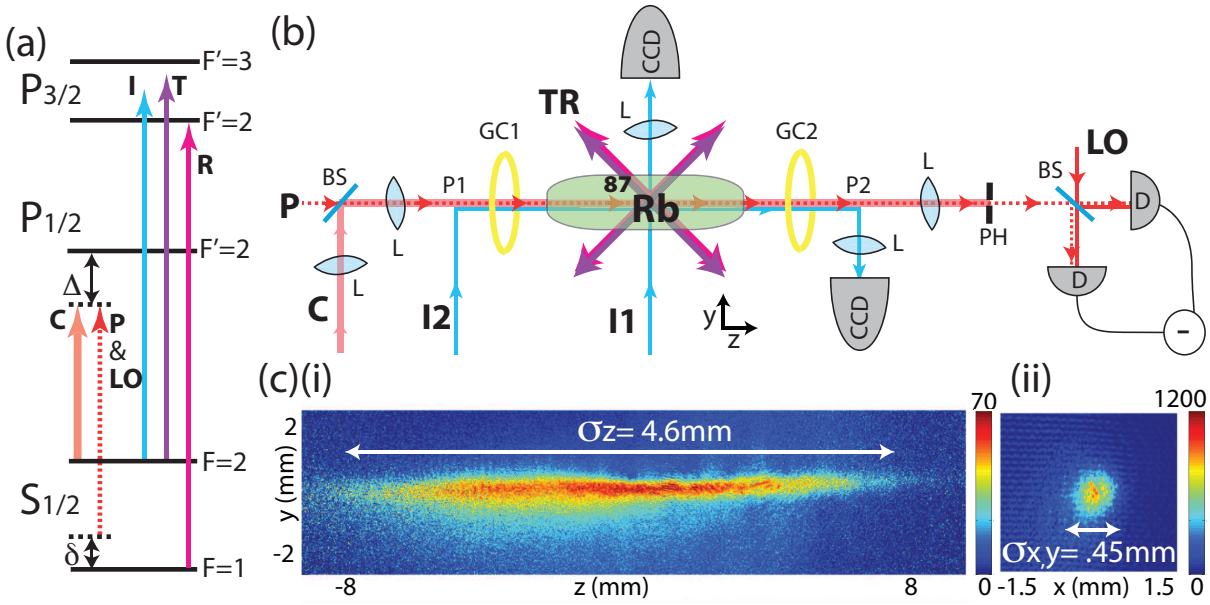

Figure 1. (a) Energy level diagram for all fields present: C - coupling; P - probe; LO - local oscillator; I - Imaging; T - trapping; R - repump. Also shown are one- and two-photon detunings for probe and coupling fields (Δ and δ respectively). (b) Experimental set-up, with: ^{87}Rb - atomic ensemble; BS - 50:50 beam-splitter; L - lens; D - photo-diode detector; I1(2) - imaging beam 1(2); CCD - charged-coupled device camera; PH - pin-hole; GC - GEM coils; P1 and P2 - positions for inserting mirrors for axial (z) imaging with I2. MOT coil configuration not shown, neither is vertical (y) MOT beam. (c)(i) Side-on and (ii) front-on images of the optimised atomic ensemble. Colour bars show OD scales, σ values show the standard deviation of Gaussian fits to ensemble.

The work-horse for cold atom experiments is the magneto-optical trap (MOT), and we used a rubidium-87 MOT as our storage medium. For quantum memory applications we aimed to produce a MOT with low atomic temperatures and a very large OD. To create as high an OD as possible we optimised both the static loading of the MOT through geometry, a spatial dark spot and optical de-pumping, followed by a compression phase using a temporal dark spot. After describing the application of these techniques, we present a characterisation of the system using near-resonance absorption imaging.

We used a basic three-beam retro-reflection configuration, with the frequencies of all lasers involved illustrated in Fig. 1(a). The trapping and cooling laser had a total power of 400 mW after spatial filtering and was red-detuned by 30 MHz from the D2 $F = 2 \rightarrow F' = 3$ transition for the loading of the MOT. The repumping field was on resonance with the D2 $F = 1 \rightarrow F' = 2$ transition.

The optimal shape for a cold atomic ensemble for use as a quantum memory is a cylinder along the direction of the memory beams to allow for maximum absorption of the probe. To create this shape while still allowing easy access for the memory beams we used four elongated coils in a quadrupole configuration to create a 2D MOT in the z direction (memory axis) and

positioned the horizontal MOT beams at 45° to the long axis of the MOT. An extra set of axial coils in the z direction created 3D confinement. The shape of the MOT could then be determined by the currents in the 2D and axial coils, as well as the relative intensities of the trapping fields.

For the loading phase, the cylindrically symmetric magnetic field gradient produced by the 2D MOT coils was 16 G/cm, and for the axial coils was 2 G/cm. The ^{87}Rb atoms were produced from a natural-mixture Rb dispenser inside a $100\times50\times50$ mm^3 single-sided, anti-reflection coated cell. This cell was attached to a vacuum system consisting of a 70 L/s ion pump supplemented by a passive titanium sublimation pump; with the dispenser running in the cell we measure a background pressure at the ion pump of 1.5×10^{-9} kPa.

The density in the trapped atomic state ($F = 2$) was limited by reabsorption of fluorescence photons within the MOT (leading to an effective outwards radiation pressure [13]). By placing a dark spot of approximately 7.5 mm in diameter in the repump, atoms at the centre of the MOT were quickly pumped into the lower ground state ($F = 1$) and became immune to this unwanted effect, allowing for a higher density of atoms in the centre of the trap, as first demonstrated in [14].

We could collect over 10^{10} atoms in this configuration. However, we found that the static MOT parameters that optimise atom number did not optimise density in the compression and cooling phase of the MOT, and we typically worked with a sample of 4×10^9 atoms.

In this second stage of the ensemble preparation we used a temporal dark spot to transiently increase the density of the sample by simultaneously increasing the trapping laser and repump detunings and increasing the magnetic field gradient [15, 16, 17]. Detuning the trapping laser created some of the conditions for polarisation-gradient cooling (PGC) [18], which could be used to achieve much colder and denser ensembles than in a standard MOT. We smoothly ramped the frequency of the trapping beam from 30 to 70 MHz below resonance, and the repump beam to 8 MHz below resonance, over a period of 20 ms. The 2D magnetic field gradient in the x and y directions was ramped up to 40 G/cm as the trapping and repump lasers are detuned. We did not ramp the axial field.

Finally, we optically pumped the atoms into the desired ground state ($F = 1$, see Fig. 1(a)) by simply turning off the repump 50 μs before the trapping beam.

Absorption imaging was used to optimise and characterise the MOT. The set-up and frequency of the imaging beams are shown in Fig. 1. We performed imaging both across (I1) and along (I2) the z axis (in which case two mirrors are temporarily placed at locations P1 and P2).

As the absorption of light by atoms away from resonance will follow a Lorentzian decay, to be able to have a precise value for OD it was important to have a well calibrated line centre. This is especially important as one goes further off resonance as the relation between on-resonance OD and off-resonance OD depends on the one-photon detuning (Δ) as follows:

$$\mathrm{OD}_{res} = \frac{\Delta^2 + \gamma^2/4}{\gamma^2/4} \ln(I_t/I_o), \tag{1}$$

where I_t is the transmitted imaging beam intensity passing through the MOT off resonance, I_o is the intensity measured without the MOT present, γ is the excited state decay rate. For Rb γ is approximately 6 MHz. To measure Δ accurately we lowered the atom number in our trap until the OD did not saturate on resonance and plotted out the resonance curve as a function of detuning to accurately locate the line centre.

An image of the optimised MOT is shown in Fig. 1(c). For this image we used a 4.98 s load time followed by 20 ms of ramping fields. All fields were then turned off and an image of the

MOT was taken 500 μs later, with a comparison image being taken 150 ms later to obtain as precise a measure of I_o as possible while ensuring no atoms were still present. As the imaging beam was on the closed D2 $F = 2 \rightarrow F' = 3$ transition, it was necessary to pump atoms back into the $F = 2$ state before these images were taken. This was achieved with a 200 μs pulse of on-resonance repump light immediately before the image. The front-on image was taken 60 MHz detuned, and the side-on image was taken 20 MHz detuned from resonance. The temperature of the MOT was approximately 200 μK.

3. Gradient Echo Memory Using Cold Atoms

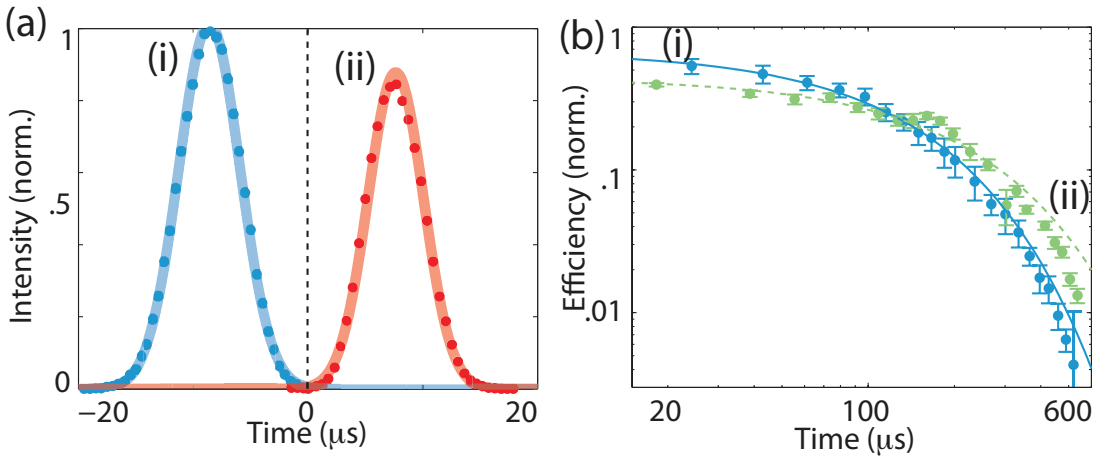

Figure 2. (a) High efficiency demodulated and squared heterodyne data: (i) input pulse (blue), and (ii) echo (red) at $80 \pm 2\%$ total efficiency. Points correspond to digitally demodulated data, averaged over 10 (17) traces for input (echo) and squared, error from standard deviation. Lines correspond to Gaussian fit. Dashed line indicates magnetic field switching at $t = 0$. (b) Memory efficiency vs storage time for storage (i) 500 μs (blue, solid) and (ii) 3 ms after MOT fields off (green, dashed).

The details of the GEM scheme are covered in depth in previous papers [1, 8, 19, 20, 21]. Here we used the three-level implementation [19], with a weak probe field and a strong coupling field, and switching magnetic field gradients produced via two solenoids, one placed either side of the MOT. This set-up and the frequencies of the fields are shown in Fig. 1(b). In the three-level implementation the effective OD is reduced by the detuning of the laser, and by the Zeeman broadening of the transition, with the final effective OD being nearly 1000-fold reduced from the on-resonance OD. This is why a high OD ensemble is critical for high efficiencies in GEM.

For the highest efficiency memory we used a 480 ms load time, and implemented the memory protocol 500 μs after the MOT fields had been turned off. We found a Gaussian pulse with a full-width-half-maximum of 10 μs to be optimal for storage. For this pulse length, a one-photon detuning of -250 MHz and approximately 350 μW in the coupling field (corresponding to a Rabi frequency of 2 MHz), we were able to demonstrate storage with $80 \pm 2\%$ total efficiency. This was measured using heterodyne detection and is shown in Fig. 2(a). As heterodyne detection is mode sensitive, care was taken to optimise the visibility for the input pulse, so that any change in the mode during storage would lead to a reduction in the measured efficiency. The coherence time for this set-up was determined to be 117 μs by storing the pulses for longer periods of time (Fig. 2(b)). By implementing the memory protocol 3 ms after the MOT had been turned off, this was increased to 195 μs.

Further improvements to the efficiency of GEM using a cold atomic ensemble could be achieved by increasing the MOT OD further, for instance by optical pumping all atoms into the correct m_F ground state. Currently the main decoherence mechanisms are not fully understood, but potentially could include inhomogeneous background magnetic fields generated via eddy currents, as well as atomic diffusion. Improving the switching electronics and physically redesigning the coil configuration could help to improve the former, while cooling the ensemble further could improve the latter.

For more information on GEM using cold atoms, see Ref. [22].

4. Conclusion

Here we have presented the development of a cold atomic ensemble with a peak OD of 1000 on the $D2$ $F = 2 \rightarrow F' = 3$ transition, and demonstrated a memory efficiency of $80 \pm 2\%$ using GEM, the highest to date using cold atoms. The primary limit on this efficiency is still the OD, which could be improved by optically pumping all the atoms into the correct m_F state. The decoherence of the system was found to be exponential, with a time constant of 117-195 μs. This is a factor of 2-4 greater than in warm vapour GEM experiments. To improve upon this, further investigations would be required to determine the limiting factors. Even without further improvement, however, our memory provides an excellent high-OD platform for numerous other proof-of-principle experiments.

Acknowledgments

Thanks to Colin Dedman for his help designing the fast switching GEM coils. This research was conducted by the *Australian Research Council Centre of Excellence for Quantum Computation and Communication Technology* (project number CE110001027). NPR is supported by an Australian Research Council QEII Fellowship. QG is supported by the AFSOR and the Physics Frontier Center at the NIST/UMD Joint Quantum Institute.

References

[1] Hosseini M, Sparkes B M, Campbell G, Lam P K and Buchler B C 2011 *Nature Commun.* **2** 174
[2] Longdell J J, Fraval E, and Sellars M J, and Manson N B 2005 *Phys. Rev. Lett.* **95** 063601
[3] Dudin Y O, Li L and Kuzmich A 2013 Light storage on the time scale of a minute *Phys. Rev. A* **87**, 031801
[4] Saglamyurek E *et al.* 2012 *Phys. Rev. Lett.* **108**, 083602
[5] Reim K F *et al.* 2010 *Nature Photon.* **4** 218-221
[6] Bonarota M, Le Gouët J-L and Chanelière T 2011 *N. J. Phys.* **13** 013013
[7] Hedges M P, Longdel J J, Li Y and Sellars M J 2010 *Nature* **465** 1052-1056
[8] Hosseini M, Sparkes B M, Hétet G, Longdell J J, Lam P K and Buchler B C 2009 *Nature* **461** 241-245
[9] Campbell G, Hosseini M, Sparkes B M, Lam P K and Buchler B C 2012 *N. J. Phys* **14** 033022
[10] Sparkes B M, Hosseini M, Cairns C, Higginbottom D, Campbell G T, Lam P K and Buchler B C 2012 *Phys. Rev. X* **2** 021011
[11] Higginbottom D, Sparkes, B M, Rancic M, Pinel O, Hosseini M, Lam P K and Buchler B C 2012 *Phys. Rev. A* **86** 023801
[12] Chen Y-H, Lee M-J, Wang I, Du S, Chen Y-F, Chen Y-C and Yu, I A 2012 *Phys. Rev. Lett.* **110** 083601
[13] Metcalf H J and van der Straten P 2003 *J. Opt. Soc. Am. B* **20** 887-908
[14] Ketterle W, Davis K B, Joffe M A, Martin A and Pritchard, D E 1993 *Phys. Rev. Lett.* **70** 2253-2256
[15] Lee H J, Adams C S, Kasevich M and Chu S 1996 *Phys. Rev. Lett.* **76** 2658-2661
[16] DePue M T, Winoto S L, Han D J and Weiss D S 2000 *Opt. Commun.* **180** 73-79
[17] Petrich W, Anderson M H, Ensher J R, Cornell E A 1994 *J. Op. Soc. Am. B* **11** 1332-1335
[18] Dalibard J and Cohen-Tannoudji C 1989 *J. Opt. Soc. Am. B* **6** 2023-2045
[19] Hétet G, Hosseini M, Sparkes B M, Oblak D, Lam P K and Buchler B C 2008 *Opt. Lett.* **33** 2323-2325
[20] Hosseini M, Campbell G, Sparkes B M, Lam P K and Buchler B C 2011 *Nature Phys.* **7** 794-798
[21] Hosseini M, Sparkes B M, Campbell G T, Lam P K, and Buchler B C 2012 *J. Phys. B* **45** 124004
[22] Sparkes B M, Bernu J, Hosseini M, Geng J, Glorieux Q, Altin P A, Lam P K, Robins N P and Buchler B C 2013 *N. J. Phys* **15**, 085027